Penerbit Akademia Baru

Journal of Advanced Research in Computing and Applications

Journal homepage:
https://akademiabaru.com/submit/index.php/arca/index
2462-1927

Theoretical Analysis of Two-Phase Mixed Convection Flow: Effects of Fluid-particle Interaction and Mass Concentration on Velocity, Temperature and Skin Friction

Nur Hazwani Zamri[1], Abdul Rahman Mohd Kasim[2,*], Mohd Haziezan Hassan[3], Tijjani Lawal Hassan[4], Syazwani Mohd Zokri[5], Nur Syamilah Arifin[6], Adeosun Adeshina Taofeeq[7]

[1] Centre for Mathematical Sciences, Universiti Malaysia Pahang Al-Sultan Abdullah, Gambang, 26300 Kuantan, Pahang, Malaysia
[2] Centre for Research in Advanced Fluid and Process, University Malaysia Pahang, Lebuhraya Tun Razak, Pahang, Gambang, 26300, Malaysia
[3] Maktab Rendah Sains MARA Kuantan, Jalan Tok Sira, Kampung Alor Akar, 25250 Kuantan, Pahang
[4] School of General Studies, Kano State Polytechnic, PMB 3401, BUK Road, Gwale, Kano, Nigeria
[5] College of Computing, Informatics and Mathematics, UiTM Terengganu Branch, Kuala Terengganu Campus, 21080 Kuala Terengganu, Malaysia
[6] College of Computing, Informatics and Mathematics, UiTM Cawangan Johor Kampus Pasir Gudang, 81750, Masai Johor, Malaysia
[7] Federal College of Education, 232102 Iwo Nigeria

ARTICLE INFO

Article history:
Received 30 December 2024
Received in revised form 21 January 2025
Accepted 9 February 2025
Available online 10 March 2025

Keywords:
Theoretical Analysis; Two-Phase Flow; Fluid-Particle Interaction; Mass Concentration; mixed convection

ABSTRACT

Research on Newtonian fluids, a fundamental area in fluid flow studies, serves as a key reference for more complex models. The deformation of fluid structure due to the presence of solid particles in Newtonian fluids necessitates a detailed analysis. Conventional models are insufficient to describe such systems, as they are categorized as two-phase fluid flows. The study of two-phase systems (fluid and solid) has gained significant attention due to its wide applications in real-life scenarios, including air and water pollution, blood flow in arteries, and coolant flow in vehicle engines. This field's high potential has driven researchers to find effective solutions to these challenges. The two-phase model not only focuses on fluid flow but also accounts for the interaction between the fluid and solid particles. This study theoretically examines a modified model that considers fluid phase and dusty phase under mixed convection of Newtonian model. Using an appropriate similarity transformation, the governing partial differential equations are converted into ordinary differential equations. The Runge-Kutta-Fehlberg method, implemented in the Maple software, is used to solve the obtained equations numerically. The results for velocity and temperature distributions, along with skin friction, are presented. The study also explores various physical parameters, including mixed convection parameter, fluid-particle interaction parameter and mass concentration parameter for both phases. The findings reveal that the presence of dust particles significantly affects the velocity and temperature behavior of both phases. Specifically, increasing particle concentration leads to a reduction in fluid velocity and temperature distribution.

* *Corresponding author.*
E-mail address: rahmanmohd@umpsa.edu.my (Abdul Rahman Mohd Kasim)

https://doi.org/10.37934/arca.38.1.1227

1. Introduction

Fluid mechanics plays a vital role in various engineering and technological processes, encompassing the study of fluid behaviour in both static and dynamic conditions. A crucial subset of fluid dynamics is the investigation of the interaction of different categories of fluids with other substances and their behaviour under the influence of external forces. Among the fluid categorizations, Newtonian and non-Newtonian fluids stand out, differing apart by their distinct viscosity behavior.

In Newtonian fluids, viscosity remains constant regardless of the applied forces, making them conducive to applications in processes such as industrial fluid transport, lubrication, and heat transfer fluids [1-3]. Another fluid classification is based on the phase of matter present in the fluid flow. This classification involves single-phase and multi-phase flow. A single phase consists of one phase, while a multi-phase flow involves multiple phases as one mixture [4]. Earlier literature focused on single phase flows, however, in recent times, multi-phase flows have gained significance as they accurately represent real-world scenarios compared to single phase [5].

A common and essential form of multi-phase flow is the two-phase fluid flow, which involves combinations of liquid-liquid, liquid-solid or gas-liquid phases. Several works on multi-phase flow have been reported in literature. For instance, Khan et al [6] investigated gas–liquid two-phase flow regime identification in a horizontal pipe and concluded that dynamic pressure signals of different flow regimes show different characteristics. Interaction between non-Newtonian Williamson fluid and dust particles were analyzed by Kasim et al [7]. They observed that Williamson fluid contributed to an increase in skin friction in flow regime.

More Interesting works on MHD and multi-phase flow can be found in established reports [8-14]. While numerous studies have investigated the behavior of Newtonian fluids and their interactions with external factors [15–20], there is a notable lack of research directly comparing the dynamics of dust-free Newtonian fluids to those containing dust particles under mixed convection conditions. This gap limits a comprehensive understanding of how dust particles influence the behavior of Newtonian fluids in such environments. To address this, the present study aims to mathematically analyze the impact of physical parameters on the Navier-Stokes equations governing both single-phase and two-phase Newtonian fluids in a mixed convection setting.

2. Methodology

The investigated flow configuration involves a two-dimensional, laminar, incompressible, and steady boundary layer flow of two Newtonian fluids, one in fluid phase and the other is a mixture of fluid phase with dust particles. The dust particles were assumed to be small, spherical, and uniformly sized solids that do not dissolve in the fluid. Both fluid flow over a vertical stretching sheet with linear velocity $u_w = ax$(a is a positive constant) and subjected to an aligned magnetic field of strength B_0 applied at an acute angle α_1 in the direction of the flow. Furthermore, a Newtonian heating condition is applied on the sheet. Under these assumptions, the governing equation for both fluids under boundary layer and Boussinesq approximations is as follows.

Fluid phase

$$\frac{\partial \overline{u}}{\partial \overline{x}} + \frac{\partial \overline{v}}{\partial \overline{y}} = 0, \tag{1}$$

$$\left(\bar{u}\frac{\partial \bar{u}}{\partial \bar{x}}+\bar{v}\frac{\partial \bar{u}}{\partial \bar{y}}\right)=\frac{\mu}{\rho}\frac{\partial^2 \bar{u}}{\partial \bar{y}^2}+\frac{\rho_p}{\rho T_v}(\bar{u}_p-\bar{u})-\frac{\sigma}{\rho}B_0^2\bar{u}\sin^2 a_1+g\beta(x)(\mathrm{T}-\mathrm{T}_\infty), \tag{2}$$

$$\left(\bar{u}\frac{\partial T}{\partial \bar{x}}+\bar{v}\frac{\partial T}{\partial \bar{y}}\right)=\alpha\frac{\partial^2 T}{\partial \bar{y}^2}+\frac{\rho_p c_s}{T_T\rho c_p}(T_p-T), \tag{3}$$

Dust phase

$$\frac{\partial \bar{u}_p}{\partial \bar{x}}+\frac{\partial \bar{v}_p}{\partial \bar{y}}=0, \tag{4}$$

$$\left(\bar{u}_p\frac{\partial \bar{u}_p}{\partial \bar{x}}+\bar{v}_p\frac{\partial \bar{u}_p}{\partial \bar{y}}\right)=-\frac{1}{T_v}(\bar{u}_p-\bar{u}), \tag{5}$$

$$\left(\bar{u}_p\frac{\partial T_p}{\partial \bar{x}}+\bar{v}_p\frac{\partial T_p}{\partial \bar{y}}\right)=-\frac{1}{T_T}(T_p-T), \tag{6}$$

with boundary conditions

$$\begin{aligned}&\bar{u}=\bar{u}_w,\ \bar{v}=0,\ \frac{\partial T}{\partial \bar{y}}=-h_s T,\ @\ \ \bar{y}=0,\\ &\bar{u}\to 0,\ \bar{u}_p\to 0,\ \bar{v}_p\to\bar{v},\ T\to T_\infty,\ T_p\to T_\infty\quad as\ \ \bar{y}\to\infty.\end{aligned} \tag{7}$$

Applying the following variables to nondimensionalize the governing equations

$$\begin{aligned}&x=\frac{\bar{x}}{L},\ y=\frac{\bar{y}}{L}\mathrm{Re}^{1/2},\ u=\frac{\bar{u}}{U_0},\ v=\frac{\bar{v}}{U_0}\mathrm{Re}^{1/2},\ u_w=\frac{\bar{u}_w}{U_0},\\ &\theta=\frac{T-T_\infty}{T_\infty},\ \theta_p=\frac{T_p-T_\infty}{T_\infty},\ T_T=\frac{3}{2}\frac{v\rho c_s T_v}{k},\alpha=\frac{k}{\rho c_p},\end{aligned} \tag{8}$$

the governing equations become

Fluid phase

$$\frac{\partial u}{\partial x}+\frac{\partial v}{\partial y}=0, \tag{9}$$

$$\left(u\frac{\partial u}{\partial x}+v\frac{\partial u}{\partial y}+\right)=\frac{\partial^2 u}{\partial y^2}+N\beta(u_p-u)-Mu\sin^2\alpha+\frac{g\beta(x)L\,\mathrm{T}_\infty}{U_0^2}\theta, \tag{10}$$

$$\left(u\frac{\partial \theta}{\partial x}+v\frac{\partial \theta}{\partial y}\right)=\frac{1}{\mathrm{Pr}}\frac{\partial^2\theta}{\partial y^2}+\frac{2}{3}\frac{\beta N}{\mathrm{Pr}}(\theta_p-\theta), \tag{11}$$

Dust phase

$$\frac{\partial u_p}{\partial x}+\frac{\partial v_p}{\partial y}=0, \tag{12}$$

$$\left(u_p\frac{\partial u_p}{\partial \overline{x}}+v_p\frac{\partial u_p}{\partial y}+\right)=-\beta(u_p-u), \tag{13}$$

$$\left(u_p\frac{\partial \theta_p}{\partial x}+v_p\frac{\partial \theta_p}{\partial y}\right)=-\frac{2}{3}\frac{\beta}{\gamma \mathrm{Pr}}(\theta_p-\theta), \tag{14}$$

with the appropriate boundary conditions

$$\begin{aligned} &u=u_w,\, v=0,\ \frac{\partial \theta}{\partial y}=-b(\theta+1)\ \ @\ \ y=0,\\ &u\to 0,\, u_p\to 0,\ v_p\to v,\, \theta\to 0,\, \theta_p\to 0\ \ as\ \ y\to\infty. \end{aligned} \tag{15}$$

In Eq. (9)-(15), $\mathrm{Pr}=\frac{\nu\rho c_p}{k}$ is Prandtl number, $\beta=\frac{L}{U_0T_v}$ is the fluid particle interaction parameter, $M=\frac{\sigma B_0^2L}{\rho U_0}$ is the magnetic field parameter, $b=\frac{h_sL}{\mathrm{Re}^{1/2}}$ is the Newtonian heating conjugate parameter, $\gamma=\frac{c_s}{c_p}$ is the specific heat ratio of the mixture and $N=\frac{\rho_p}{\rho}$ is the mass concentration of the particles.

Seeking similarity solution of the problem, we implement the similarity transformation defined as follows.

$$\eta=y,\, u=xf'(\eta),\, u_p=xF'(\eta),\, v=f(\eta),\, v_p=F(\eta),\, \beta(x)=\beta_0x,\, u_w=x, \tag{16}$$

where η is the similarity variable, $f(\eta), F(\eta)$ are respective dimensionless fluid velocity and dust particle velocity, β_0 is the constant thermal buoyancy term. The following ordinary differential equations (14)-(16) are obtained by substituting Eq. (13) into (9)-(12).

$$f'''+ff''-f'^2+N\beta(F'-f')-Mf'\sin^2\alpha+\lambda\theta=0, \tag{17}$$

$$\frac{1}{\mathrm{Pr}}\theta''+f\theta'+\frac{2}{3}\beta N(\theta_p-\theta)=0, \tag{18}$$

$$F'^2-F''F+\beta(F'-f')=0, \tag{19}$$

$$\theta_p F - \frac{2}{3\,\mathrm{Pr}\,\gamma}\frac{\beta}{(\theta_p - \theta)} = 0, \tag{20}$$

with dimensionless boundary conditions

$$\begin{aligned} &f' = 1,\ f = 0,\ \theta' = -b(1+\theta), && \text{at} \quad \eta = 0, \\ &f' \to 0,\ F' \to 0, F \to f,\ \theta \to 0,\ \theta_p \to 0 && \text{as} \quad \eta \to \infty, \end{aligned} \tag{21}$$

Here, the prime symbol stands for derivative with respect to η. $\lambda = \frac{Gr}{\mathrm{Re}^2}$ is the mixed convection parameter, $Gr = \frac{g\beta_0 L^3 T_\infty}{\nu^2}$ is Grashof number and $\mathrm{Re} = \frac{U_0 L}{\nu}$ is Renold's number.

3. Results

Equations (17) to (20) were solved using a numerical approach, specifically employing the Runge-Kutta-Fehlberg method, which is a higher-order numerical technique known for its efficiency in solving ordinary differential equations (ODEs). This method was implemented using Maple Software, a powerful computational tool for symbolic and numerical analysis. To assess the effects of various parameters—such as fluid-particle interactions, magnetic fields, mixed convection, and particle concentration—on key flow characteristics like skin friction, velocity profiles, and temperature distributions, the system of equations was numerically integrated. These parameters play significant roles in determining the behavior of the fluid-particle mixture, affecting how momentum and heat are transferred within the flow. Before proceeding with the solutions, a validation process was carried out to ensure the accuracy and reliability of the current model. This step typically involves comparing the numerical results with known analytical solutions or benchmark data from previous studies. Validation is crucial for confirming that the model correctly represents the physical phenomena and that the numerical approach, including the chosen method and software, produces credible results under the specified conditions. This ensures the robustness of the model for further analysis of the effects of the varying parameters on the fluid-particle system. Table 1 and Figure 1 provide a comparative representation of the skin friction results in the limiting case for different approaches.

Table 1
Comparative values of skin friction coefficient, $-f''(0)$, for various values of M when $N = \beta = \lambda = 0$, $\alpha_1 = \pi/2$, $\gamma = \infty$

M	Exact Equation	Fathizadeh *et al.,* [21]	Present
0	1.00000	1.00000	1.00048
1	1.41421	1.41421	1.41422
5	2.44949	2.44948	2.44949
10	3.31662	3.31662	3.31662
50	7.14143	7.14142	7.14143
100	10.04988	10.04998	10.04988

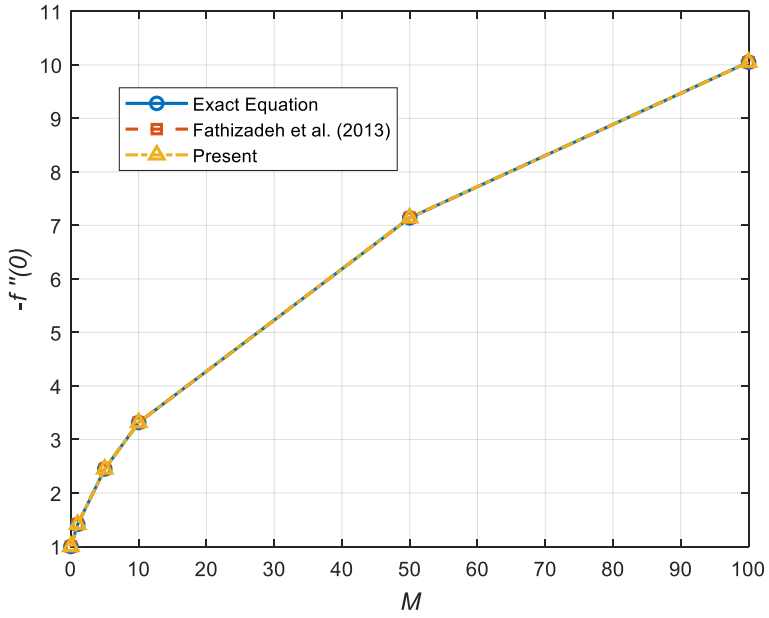

Fig. 1. Comparative representation of the skin friction results

These results offer a clear visualization of the variations in skin friction across the different methods under specific conditions, allowing for an in-depth comparison of the approaches and their effectiveness in capturing the limiting behavior of skin friction. The results are analyzed based on accuracy, consistency, and performance across the range of the constant value of magnetic field, *M*. The Present method demonstrates superior accuracy and consistency, matching the Exact Equation almost perfectly across all *M*. In 2013, *Fathizadeh et al.,* [21] provides reliable results but shows slightly larger deviations, particularly at intermediate values of *M.* These results affirm the robustness and reliability of the present method as a computational tool for solving the respective problem. Therefore, the Runge-Kutta approach may be reckoned upon to be effective in resolving the dusty fluid flow problem. In this investigation we are interested to focus on behaviour of skin friction in the present of parameter Fluid-particle interaction parameter, β, Magnetic field parameter, *M*, and Mixed convection parameter, λ.

Table 2
Values of skin friction coefficient, $f''(0)$, for various values of β when $Pr = 7, b = 0.001, \lambda = 0.5, N = 0.5, \gamma = 0.1, M = 1$, $\alpha_1 = \pi/6$

β	$f''(0)$
0	-1.1202466
1	-1.1381802
5	-1.1902372
10	-1.2247432

Based on the result shown, it can be observed that the value of the skin friction, $f''(0)$, is decreasing with increase in the fluid particle interaction, β. The strong interactions between fluid particles can reduce skin friction by promoting laminar flow, increasing viscosity, suppressing turbulence, and enhancing the flow's organization. These effects lead to a smoother, more controlled fluid interaction with the surface, reducing the drag and, therefore, the skin friction. Figures 2 and 3

illustrate the velocity distribution for both the fluid and dust phases. The data clearly indicate that strong interactions between the particles result in contrasting behaviors for the fluid and dust velocities. Specifically, as the interaction between particles intensifies, the velocity of the fluid decreases, while the velocity of the dust phase exhibits an opposite trend, increasing in response to the stronger particle interactions. This inverse relationship highlights the distinct dynamics of the fluid and dust phases under varying interaction conditions.

Figures 4 and 5 illustrate the temperature profiles for the fluid and dust phases respectively. As β increases, the temperature profile for the dust phase increases, while that of the fluid phase decreases. This contrasting behavior can be attributed to the velocity relaxation time of the dust phase in response to an increase β.

When β increases, the dust phase becomes denser, leading to stronger particle-particle and particle-fluid interactions. These interactions increase the time required for the dust phase to reach equilibrium with the fluid phase, resulting in the accumulation of thermal energy within the dust phase and, consequently, an increase in its temperature profile. Conversely, for the fluid phase, the higher β extracts more energy from the fluid via momentum and thermal coupling. This energy transfer reduces the fluid's overall thermal energy, causing its temperature profile to decrease. The differences in how the two phases respond to increased β are thus closely tied to the dust phase's slower velocity relaxation and its ability to retain more heat in comparison to the fluid phase.

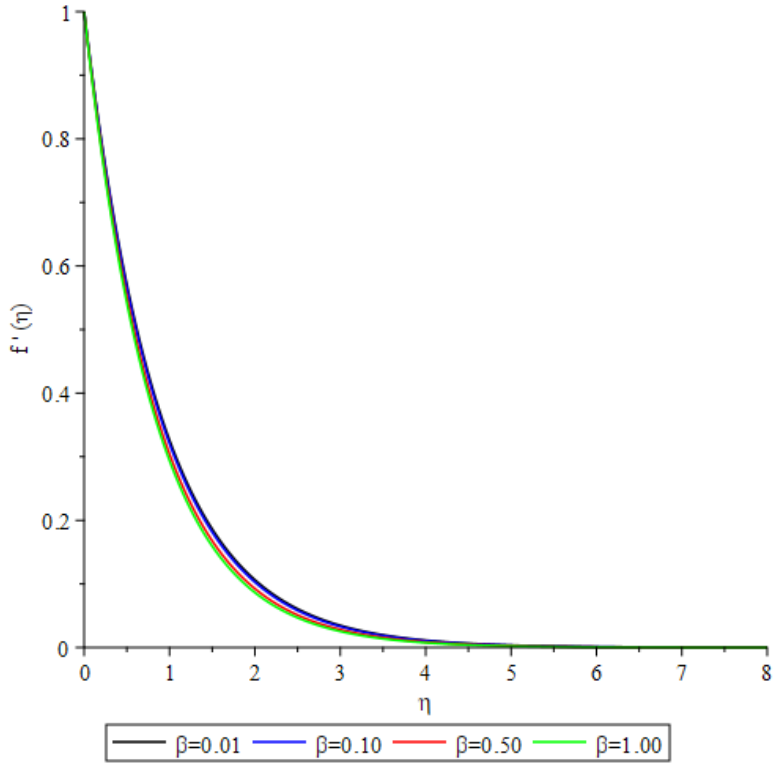

Fig. 2. Velocity profile for fluid phase with various β and $Pr = 7, b = 0.001, \lambda = 0.5, N = 0.5, \gamma = 0.1, M = 1,$ and $\alpha_1 = \pi/6$

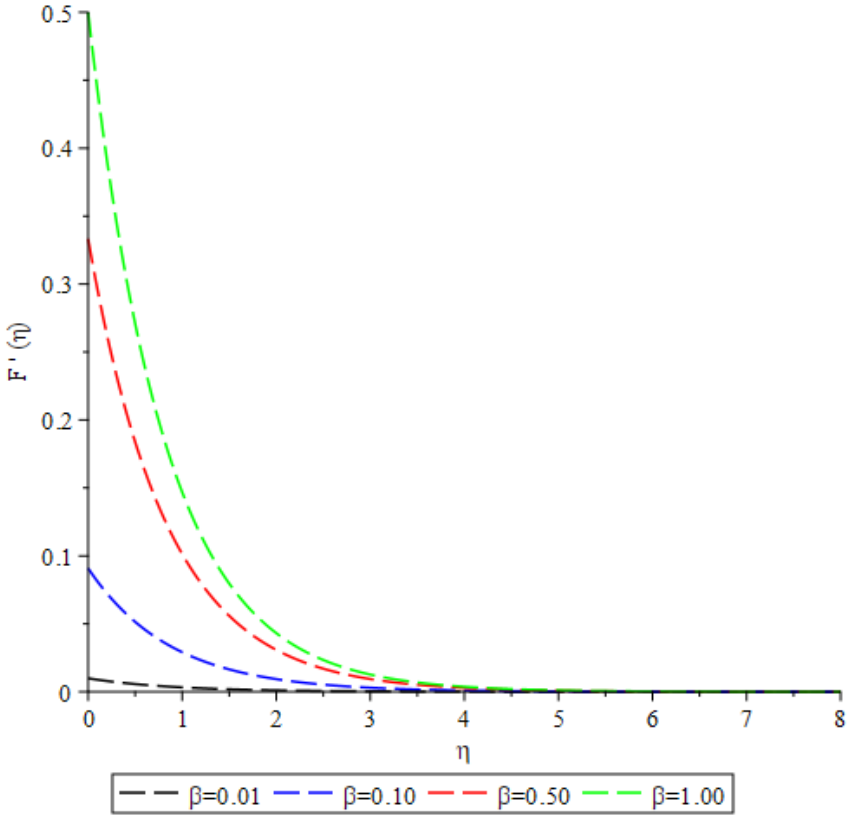

Fig. 3. Velocity profile for dust phase with various β and $Pr = 7, b = 0.001, \lambda = 0.5, N = 0.5, \gamma = 0.1, M = 1$, and $\alpha_1 = \pi/6$

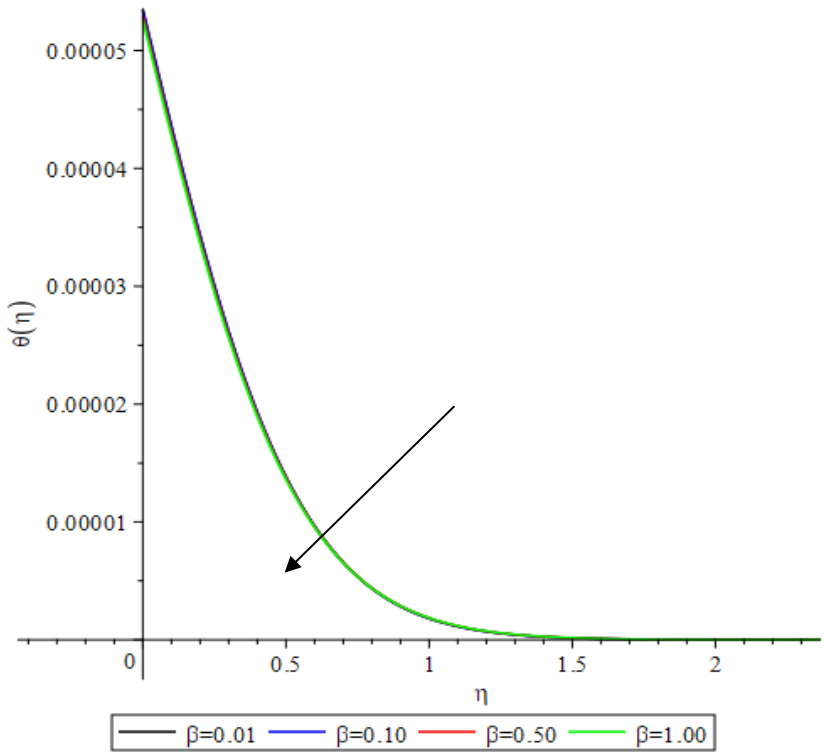

Fig. 4. Temperature profile for fluid phase with various β and $Pr = 7, b = 0.001, \lambda = 0.5, N = 0.5, \gamma = 0.1, M = 1$, and $\alpha_1 = \pi/6$

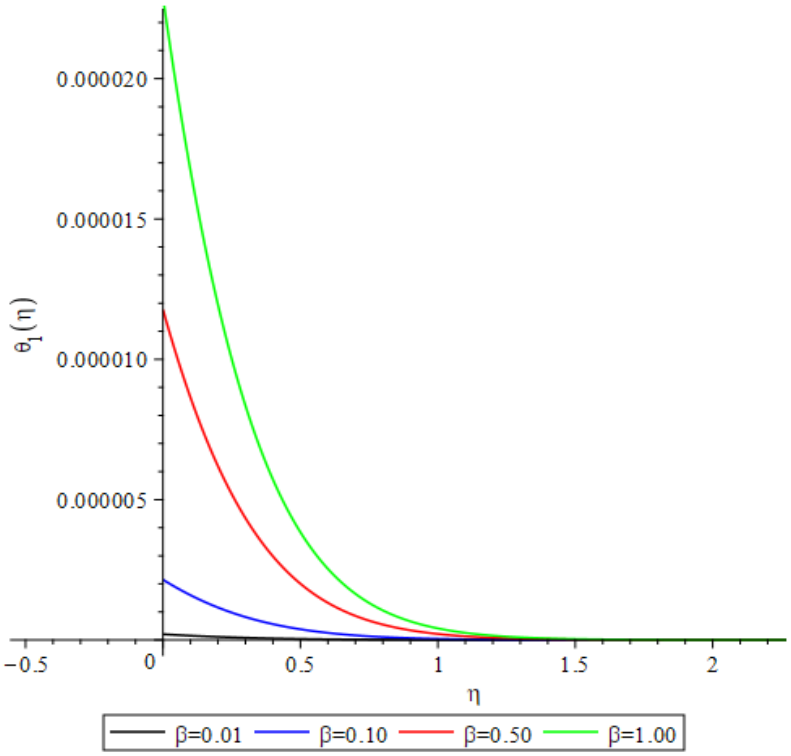

Fig. 5. Velocity profile for dust phase with various β and $Pr = 7, b = 0.001, \lambda = 0.5, N = 0.5, \gamma = 0.1, M = 1,$ and $\alpha_1 = \pi/6$

The values presented in Table 3 show the skin friction variations with different values of the mixed convection parameter, λ. As indicated by the data and the graph, the skin friction behaves in a rather unpredictable manner with no clear trend, especially as λ increase. This unpredictability suggests a complex interaction between the fluid and solid phases under varying conditions of λ. While the skin friction does not follow a uniform pattern, it is essential to note that this non-uniform behavior could be attributed to changes in flow dynamics, energy dissipation, and boundary layer development, influenced by the λ.

Table 3
Values of skin friction coefficient, $f''(0)$, for various values of λ when $Pr = 7, b = 1, \alpha = \frac{\pi}{6}, N = 0.5, \gamma = 0.01, M = 1, \beta = 0.01$

λ	$f''(0)$
0.0	-1.1202534
0.2	-1.0627019
5.0	-0.0248984
10.0	-0.8847447

The unpredictable trend in skin friction directly influences the velocity profiles of both the fluid and dust phases (refer Figure 6 and 7) due to the coupling between shear forces, flow dynamics, and momentum transfer within the boundary layer. Skin friction arises from the tangential shear stress at the surface, which governs how momentum is transferred between the solid boundary and the fluid-dust mixture. Variations in skin friction disrupt this momentum exchange, leading to irregularities in velocity distribution. Meanwhile the temperature profiles for both the fluid and dust

phases decrease with an increase in the λ. as shown in Figures 8 and 9. This behavior occurs because a higher λ contributes to stronger influence of forced convection relative to natural convection. In forced convection-dominated flows, the fluid moves more rapidly, which reduces the time available for heat transfer between the surface and the surrounding fluid, leading to thinner thermal boundary layers. Consequently, the temperature gradients near the surface decrease, resulting in lower temperature profiles for both phases. Additionally, the dust phase, which depends on heat transfer from the fluid, mirrors this trend, as the reduced thermal energy in the fluid phase limits the heat available for transfer to the dust particles. This combined effect explains the observed decrease in temperature profiles with increasing λ.

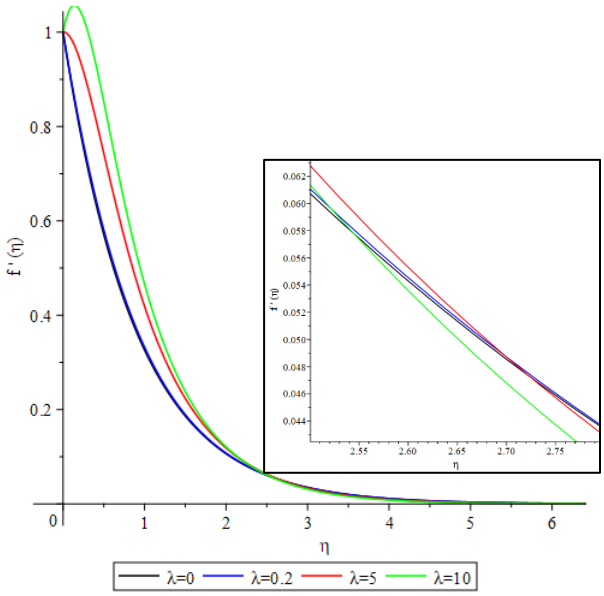

Fig. 6. Velocity profile for fluid phase with various λ and $Pr = 7, b = 1, \alpha_1 = \frac{\pi}{6}, N = 0.5, \gamma = 0.01, M = 1$, and $\beta = 0.01$

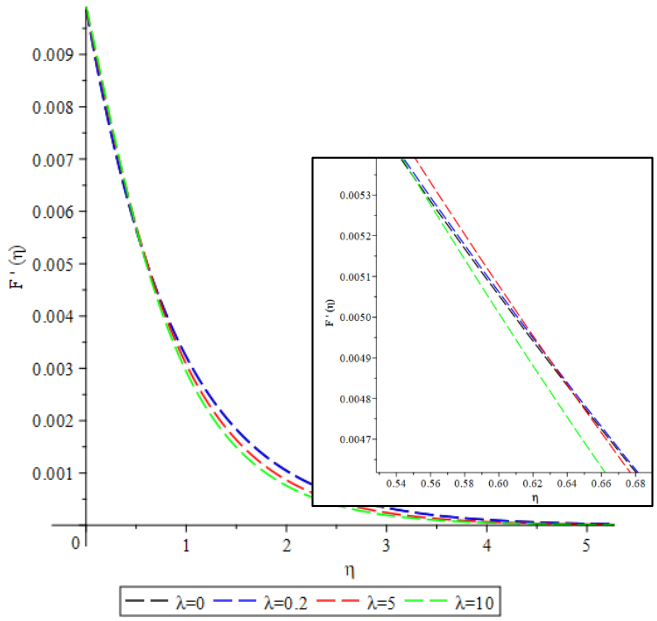

Fig. 7. Velocity profile for dust phase with various λ and $Pr = 7, b = 1, \alpha_1 = \frac{\pi}{6}, N = 0.5, \gamma = 0.01, M = 1$, and $\beta = 0.01$

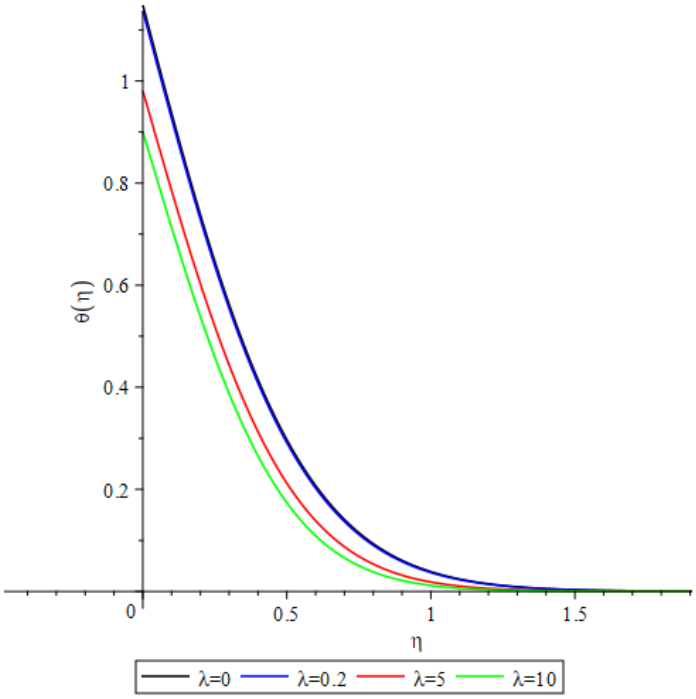

Fig. 8. Temperature profile for fluid phase with various λ and $Pr = 7, b = 1, \alpha_1 = \frac{\pi}{6}, N = 0.5, \gamma = 0.01, M = 1$, and $\beta = 0.01$

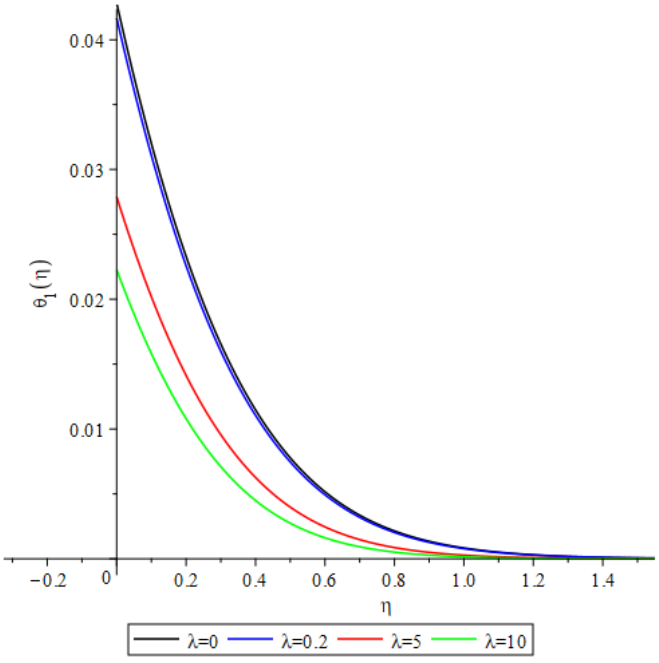

Fig. 9. Temperature profile for dust phase with various λ and $Pr = 7, b = 1, \alpha_1 = \frac{\pi}{6}, N = 0.5, \gamma = 0.01, M = 1$, and $\beta = 0.01$

As shown in Table 5, the value of skin friction decreases with an increasing in the mass concentration of the particle, *N*. This trend can be attributed to the factor of momentum dilution effect where the increasing *N* offer a higher concentration of dust particles into the fluid, effectively diluting the momentum transfer within the fluid phase while the dust particles absorb and dissipate energy from the fluid, reducing the shear stress at the wall and, consequently, lowering the skin friction. The trend of decreasing skin friction under larger *N* is also due to the reduction in Fluid Phase Dominance which caused in thicken the dust concentrations and reduce the relative influence of the fluid phase, weakening its ability to transfer momentum effectively through the boundary layer. This results in a lower velocity gradient near the surface, which corresponds to reduced skin friction. As *N* increases, the velocity profiles for both the fluid and dust phases decrease, as indicated in Figures 10 and 11. This behavior is primarily due to the increased drag forces caused by stronger interactions between particles and between the fluid and particle phases, which decelerate both phases. Additionally, the presence of more particles enhances flow resistance, reducing the overall momentum transfer, particularly in the dust phase. Furthermore, the fluid phase loses momentum to the particle phase through interphase interactions, while the increased drag forces further slowdown the dust phase. These combined effects result in lower velocities for both phases as *N* increases.

Table 5
Values of skin friction coefficient, $f''(0)$, for various values of N when $Pr = 7, \lambda = 0.8, \alpha = \frac{\pi}{2}, b = 0.001, \gamma = 0.01, M = 1, \beta = 0.01$

N	$f''(0)$
0.01	-1.4141373
10	-1.4486861
100	-1.7290917
1000	-3.4497396

Figures 12 and Figures 13 show the variation of temperature profile for both phases with different values of N. In Figure 12, it shows that the temperature profile for fluid phase decreases with an increase in N values. However, for the dust phase, increase values of N show increasing pattern for the temperature profile.

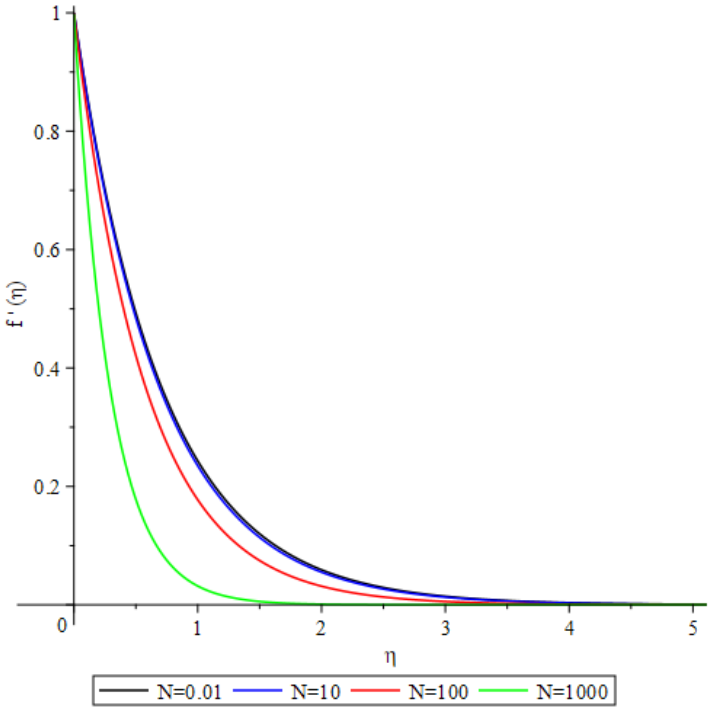

Fig. 10. Velocity profile for fluid phase with various N and $Pr = 7, b = 0.001, \alpha_1 = \frac{\pi}{2}, \lambda = 0.8, \gamma = 0.01, M = 1,$ and $\beta = 0.01$

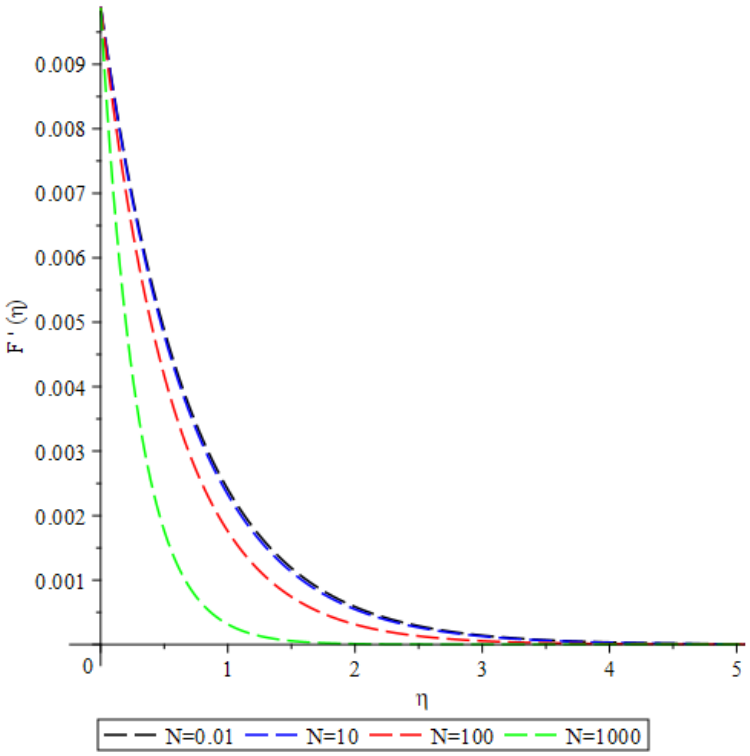

Fig. 11. Velocity profile for dust phase with various $N$and $Pr = 7, b = 0.001, \alpha_1 = \frac{\pi}{2}, \lambda = 0.8, \gamma = 0.01, M = 1,$ and $\beta = 0.01$

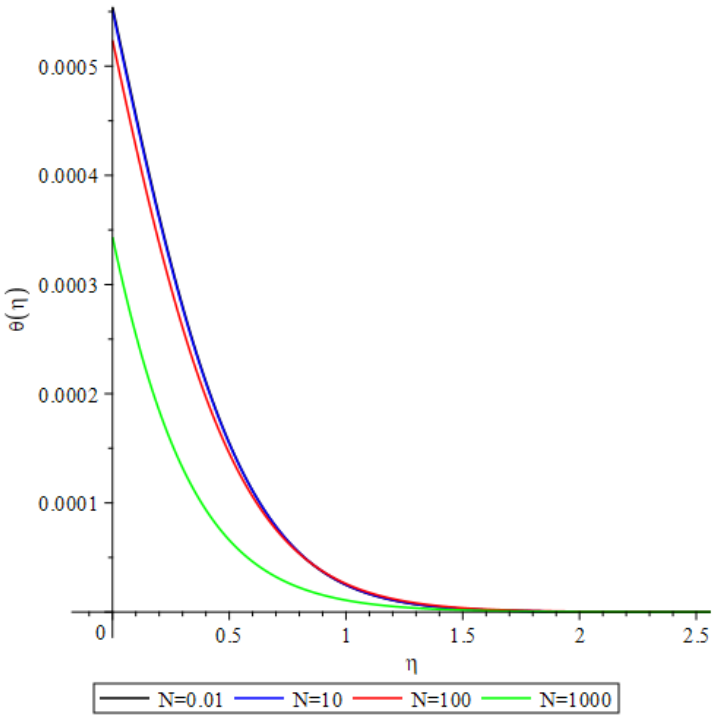

Fig. 12. Temperature profile for fluid phase with various $N$and $Pr = 7, b = 0.001, \alpha_1 = \frac{\pi}{2}, \lambda = 0.8, \gamma = 0.01, M = 1,$ and $\beta = 0.01$

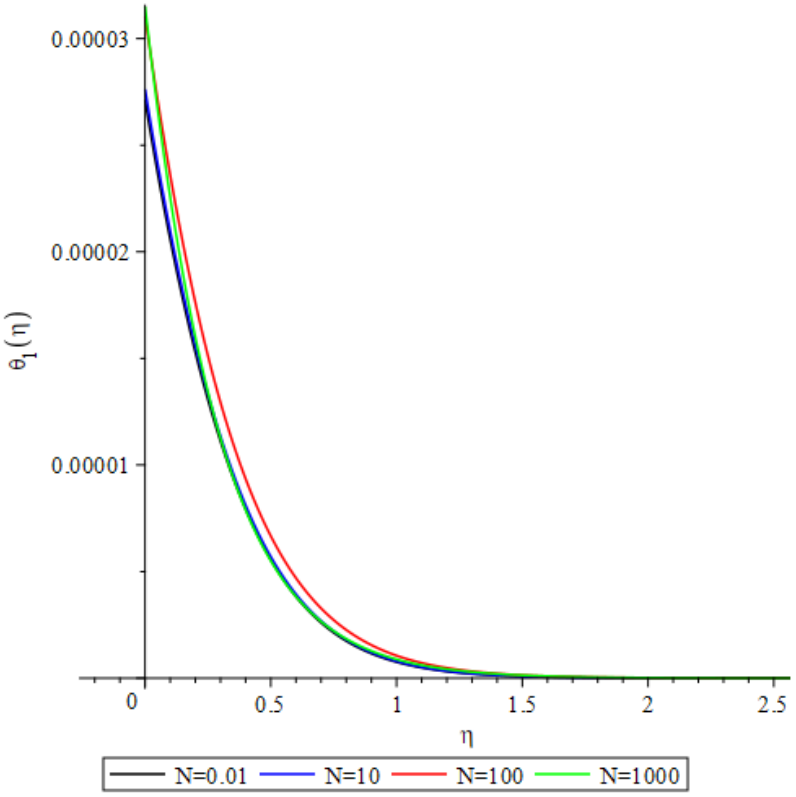

Fig. 13. Temperature profile for dust phase with various $N$and $Pr = 7, b = 0.001, \alpha_1 = \frac{\pi}{2}, \lambda = 0.8, \gamma = 0.01, M = 1,$ and $\beta = 0.01$

4. Conclusions

This study provides an analysis of the behaviour of a Newtonian fluid and dust particles under mixed convection, focusing on skin friction, velocity profiles, and temperature distributions influenced by few significant parameters. The results reveal that fluid-particle interactions, magnetic fields, mixed convection effects, and particle concentration significantly affect the flow dynamics and thermal characteristics of the system. Key findings indicate that stronger fluid-particle interactions reduce fluid velocity and skin friction while enhancing dust phase velocity and temperature. Conversely, increased particle concentration lowers the velocities of both phases and reduces skin friction due to enhanced drag forces and momentum dilution. Mixed convection introduces complex variations in flow and thermal behaviour, emphasizing the interplay between natural and forced convection. The robustness and accuracy of the present computational approach highlight its effectiveness in modelling such complex multiphase systems, offering valuable insights for applications in fluid mechanics and heat transfer.

Acknowledgement

The authors sincerely acknowledge Universiti Malaysia Pahang Al-Sultan Abdullah for the financial support provided under research grant RDU233204. Appreciation is also extended to Universiti Teknologi MARA (UiTM) Johor Branch, Universiti Teknologi MARA (UiTM) Terengganu Branch, Kano State Polytechnic, and the Federal College of Education Iwo, Nigeria, for their invaluable guidance and support.

References

[1] Bird, R. Byron, Warren E. Stewart, and Edwin N. Lightfoot. "Transport Phenomena 2nd edition,(2002)."

[2] Bansal, Shubham, and Rajendra Singh Yadav. "Effect of slip velocity on Newtonian fluid flow induced by a stretching surface within a porous medium." *Journal of Engineering and Applied Science* 71, no. 1 (2024): 153. https://doi.org/10.1186/s44147-024-00481-z

[3] Bhandari, D. S., Dharmendra Tripathi, and J. Prakash. "Insight into Newtonian fluid flow and heat transfer in vertical microchannel subject to rhythmic membrane contraction due to pressure gradient and buoyancy forces." *International Journal of Heat and Mass Transfer* 184 (2022): 122249. https://doi.org/10.1016/j.ijheatmasstransfer.2021.122249

[4] Mazumder, Quamrul H. "CFD analysis of single and multiphase flow characteristics in elbow." *Engineering* 4, no. 4 (2012): 210-214. https://doi.org/10.4236/eng.2012.44028

[5] Arifin, Nur Syamilah, Syazwani Mohd Zokri, Abdul Rahman Mohd Kasim, Mohd Zuki Salleh, W. N. S. W. Yusoff, Nurul Farahain Mohammad, and Sharidan Shafie. "Aligned magnetic field on dusty Casson fluid over a stretching sheet with Newtonian heating." *Malaysian Journal of Fundamental and Applied Sciences* 13, no. 3 (2017): 245-248. https://doi.org/10.11113/mjfas.v13n3.592

[6] Khan, Umair, William Pao, and Nabihah Sallih. "Numerical gas–liquid two-phase flow regime identification in a horizontal pipe using dynamic pressure data." *Applied Sciences* 13, no. 2 (2023): 1225. https://doi.org/10.3390/app13021225

[7] Mohd Kasim, Abdul Rahman, Nur Syamilah Arifin, Syazwani Mohd Zokri, Noor Amalina Nisa Ariffin, and Sharidan Shafie. "How fluid particle interaction affects the flow of dusty Williamson fluid." *Symmetry* 15, no. 1 (2023): 203. https://doi.org/10.3390/sym15010203

[8] Kalpana, Gajendran, and Salman Saleem. "Heat transfer of magnetohydrodynamic stratified Dusty fluid flow through an inclined irregular porous channel." *Nanomaterials* 12, no. 19 (2022): 3309. https://doi.org/10.3390/nano12193309

[9] Shuaib, Muhammad, Tariq Saeed, Muhammad Umair, Asif Ullah, and Nejla Mahjoub Said. "Gyrotactic micro-organism dusty fluid flow over an extended surface." *Ain Shams Engineering Journal* 15, no. 12 (2024): 103119. https://doi.org/10.1016/j.asej.2024.103119

[10] Alarabi, T. H., A. Mahdy, S. S. Alzahrani, and Omima A. Abo-zaid. "Dusty non-Newtonian nanofluid flow along a stretching curved sheet via chemically reactive and heat source/sink imapct: Two-phase model." *Partial Differential Equations in Applied Mathematics* 9 (2024): 100646. https://doi.org/10.1016/j.padiff.2024.100646

[11] Kumar, Vasa Vijaya, M. N. Shekar, and Shankar Goud Bejawada. "Heat and mass transfer significance on MHD flow over a vertical porous plate in the presence of chemical reaction and heat generation." *CFD Lett* 16, no. 5 (2024): 9-20. https://doi.org/10.37934/cfdl.16.5.920

[12] Ali, Gohar, and Poom Kumam. "An exploration of heat and mass transfer for MHD flow of Brinkman type dusty fluid between fluctuating parallel vertical plates with arbitrary wall shear stress." *International Journal of Thermofluids* 21 (2024): 100529. https://doi.org/10.1016/j.ijft.2023.100529

[13] Qureshi, Imran Haider, M. Nawaz, M. A. Abdel-Sattar, Shaban Aly, and Muhammad Awais. "Numerical study of heat and mass transfer in MHD flow of nanofluid in a porous medium with Soret and Dufour effects." *Heat Transfer* 50, no. 5 (2021): 4501-4515. https://doi.org/10.1002/htj.22085

[14] Low, Euwing, Syahira Mansur, Yaan Yee Choy, and Eugene Low. "Flow and heat transfer of MHD dusty nanofluid toward moving plate with convective boundary condition." *Journal of Advanced Research in Fluid Mechanics and Thermal Sciences* 89, no. 2 (2022): 43-55. https://doi.org/10.37934/arfmts.89.2.4355

[15] Metzner, A. B., R. H. Feehs, Hector Lopez Ramos, R. E. Otto, and J. D. Tuthill. "Agitation of viscous Newtonian and non-Newtonian fluids." *AIChE Journal* 7, no. 1 (1961): 3-9. https://doi.org/10.1002/aic.690070103

[16] Liao, Shi-Jun. "On the analytic solution of magnetohydrodynamic flows of non-Newtonian fluids over a stretching sheet." *Journal of Fluid Mechanics* 488 (2003): 189-212. https://doi.org/10.1017/S0022112003004865

[17] Xu, Hang, and Shi-Jun Liao. "Series solutions of unsteady magnetohydrodynamic flows of non-Newtonian fluids caused by an impulsively stretching plate." *Journal of Non-Newtonian Fluid Mechanics* 129, no. 1 (2005): 46-55. https://doi.org/10.1016/j.jnnfm.2005.05.005

[18] Chen, Yu-Shao, Chia-Chang Lin, and Hwai-Shen Liu. "Mass transfer in a rotating packed bed with viscous Newtonian and non-Newtonian fluids." *Industrial & engineering chemistry research* 44, no. 4 (2005): 1043-1051. https://doi.org/10.1021/ie0499409

[19] Hakeem, AK Abdul, S. Saranya, and B. Ganga. "Comparative study on Newtonian/non-Newtonian base fluids with magnetic/non-magnetic nanoparticles over a flat plate with uniform heat flux." *Journal of Molecular Liquids* 230 (2017): 445-452. https://doi.org/10.1016/j.molliq.2016.12.087

[20] Yadav, Pramod Kumar, Sneha Jaiswal, Amit Kumar Verma, and Ali J. Chamkha. "Magnetohydrodynamics of immiscible Newtonian fluids in porous regions of different variable permeability functions." *Journal of Petroleum Science and Engineering* 220 (2023): 111113. https://doi.org/10.1016/j.petrol.2022.111113

[21] Fathizadeh, M., M. Madani, Yasir Khan, Naeem Faraz, Ahmet Yıldırım, and Serap Tutkun. "An effective modification of the homotopy perturbation method for MHD viscous flow over a stretching sheet." *Journal of King Saud University-Science* 25, no. 2 (2013): 107-113. https://doi.org/10.1016/j.jksus.2011.08.003